CHAPTER 4

Characterization Methods

4.1 X-Ray Powder Diffractometry

4.1.1 Introduction

The phase composition and the degree of crystallinity of the ZIO powder samples were studied using a Philips X'Pert MPD X-Ray Diffractometer. The diffraction pattern was obtained by scanning the powder sample from 10-80° 2θ angle at a step size of 0.02° and a count time of 1.5 s at each step. A Cu-Kα (λ = 1.54056 Å) tube operated at 30 kV and 40 mA was used for the generation of X-rays.

4.1.2 Principle

X-ray diffraction works on the principle of x-ray beams being diffracted by the planes that exist within the powdered sample. The phenomena can be visualized more clearly in the schematic diagram in Fig. 4.1.

When a parallel, monochromatic and coherent beam of x-rays with wavelength λ is directed on two parallel planes of atoms at an angle of θ, wave 1 is scattered by atom A while wave 2 is scattered by atom B. Both waves stay in phase after being scattered, if the path length difference between 1-A-1' and 2-B-2' (which is the length of CB + BD) is equal to a whole number of wavelengths (n). The condition for constructive interference of the scattered rays or diffraction is governed by Bragg's Law [63]. The Bragg equation is given in Equation 4.1 where d is the spacing between adjacent crystal planes and θ is the angle of scattering as defined in Fig. 4.1. Standard procedure for analyzing the diffraction patterns of powder samples involves the use of n=1 in the equation [63]:

$$n\lambda = 2d \sin\theta \quad \ldots\ldots \quad \text{(Equation. 4.1)}$$

Polycrystalline powder materials provide an infinite number of crystallite configurations that can satisfy Bragg's Law by virtue of its different d-spacings. The software plots angular positions (2θ) against intensities of resultant diffraction peaks to produce a pattern, which acts as a fingerprint of a sample. Identification of an unknown compound can be made by comparing its interplanar spacings (d-spacings) and intensities with standard powder diffraction patterns, from the Powder Diffraction File (PDF) maintained by the Joint Committee on Powder Diffraction Standards (JCPDS).

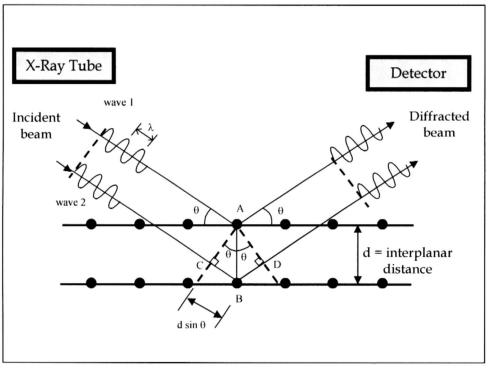

Fig. 4.1: Diffraction of x-ray beams by planes of atoms, as governed by Bragg's Law.

Apart from identification, the crystallite size of a sample can also be determined from the diffraction pattern if appreciable broadening of the peaks is observed. These broadenings may correspond to the actual size of the particles. This usually occurs when crystallites are less than 100 nm in size. The extent of broadening is described by β, which is the full width at half maximum intensity of the peak, as illustrated in Fig. 4.2.

After the value of β (in radians) is corrected for the instrumental contribution, it can be substituted into Scherrer's equation [64]:

$$D = \frac{0.9\lambda}{\beta \cos\theta_{\beta}} \quad \ldots\ldots \quad \text{(Equation 4.2)}$$

where D is the crystallite diameter, λ is the wavelength and θ_{β} is the diffraction angle. The factor 0.9 comes about as an approximation of the angle $2\theta_{\beta}$ at the maximum intensity of I_{max}.

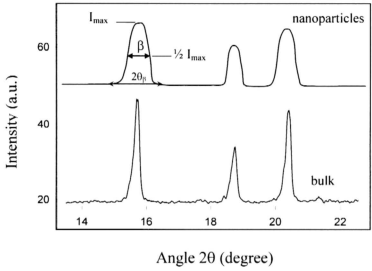

Fig. 4.2: Diffraction patterns of a nanocrystalline material showing broadening because of particle size.

4.1.3 Sample Preparation

The sample is first crushed and ground using agate mortar. A few milligrams of the powdered sample were placed onto a specially cut silicon disc before it is inserted into the sampling chamber of the diffractometer. The sample can also be placed onto glass slides instead of the more expensive silicon discs, but the silicon discs have the advantage of not producing diffraction pattern or background noise. This enables a clearer diffraction pattern originating only from the powdered sample.

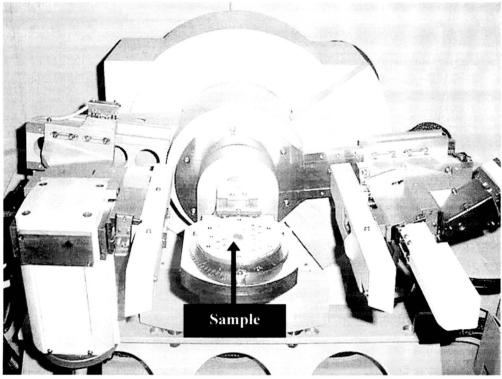

Fig. 4.3: Sample chamber of XRD where the sample is subjected to x-rays.

4.2 Alternating Gradient Magnetometry

4.2.1 Introduction

The behavior of the samples under a magnetic field was investigated using a MicroMag 2900 alternating gradient magnetometer (AGM) from Princeton Measurements Corporation. This equipment is highly sensitive and capable of measuring magnetic properties on a wide range of sample types and strengths, such as coercivity, saturation magnetization and remanence.

4.2.2 Principle

The AGM utilizes an alternating gradient field to exert a force on a sample, resulting in a deflection of the sample within the field. This deflection is measured by a piezoelectric sensing element mounted on the probe arm. The electrical signals are processed by a computer, which is linked to the magnetometer. Analysis of the magnetic properties is performed by a software package.

The sample is mounted on an extension rod attached to the piezoelectric element, as shown in Fig. 4.4. The transducer probe is attached to a stage situated between two electromagnets, as can be seen in Fig. 4.5. A gradient field strength alternating from a maximum of 10kOe to a minimum of –10kOe was exerted on the sample.

4.2.3 Sample Preparation

About 0.3-0.8 μg of powdered sample was weighed prior to placement on a $9mm^2$ piece of double-sided tape. This specimen is then stuck onto the sample carrier on the transducer probe using silicon grease. The transducer probe is then fitted onto the AGM and measurement was performed.

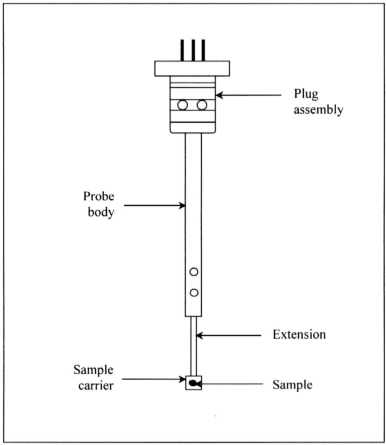

Fig. 4.4: The transducer probe on which the sample is mounted.

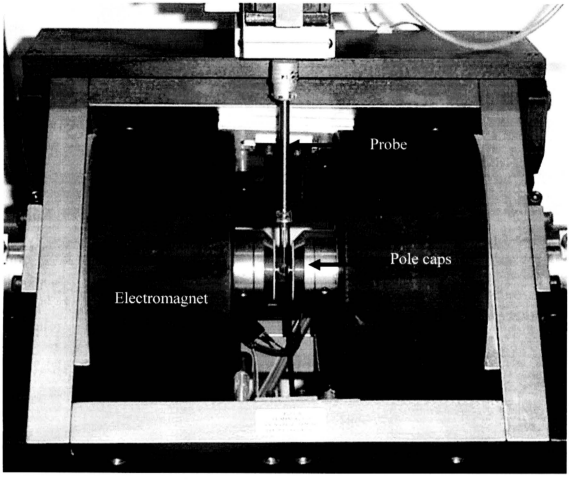

Fig. 4.5: The set-up of the transducer probe within the magnetometer assembly.

4.3 Scanning Electron Microscopy and Energy Dispersive X-Ray Spectrometry

4.3.1 Introduction

The size and surface morphology of the powder particles were observed under a Philips XL40 scanning electron microscope (SEM) while a semi-quantitative elemental analysis was performed using an energy dispersive X-ray spectrometer (EDS) 10-litre detecting unit from EDAX that was combined with the SEM. The two techniques of electron-optical imaging and X-ray microanalysis were first combined in the late 1940s [65]. The EDS detector has a narrow diameter end cap with a fixed window that separates the internal components and vacuum of the detecting unit from the scanning electron microscope chamber. The unit can be configured for light element analysis down to beryllium (atomic number 4).

The SEM uses electrons instead of light waves to form an image. In comparison with a light microscope, electrons have smaller wavelengths, so images of better resolution are produced by an SEM. This is useful for mapping details of objects. The image is presented in grayscale.

4.3.2 Principle

When an electron beam strikes a solid specimen, a number of interactions occur, with the most important of these illustrated in Fig. 4.6. Electrons may be back-scattered from the front face of the specimen with little or no energy loss, or they may interact with surface atoms to produce secondary, low energy electrons. Some electrons may be absorbed by the specimen with transfer of energy to heat and sometimes to light, while transmitted electrons may be unchanged in direction or scattered at different angles. Scattered electrons may be elastic (no energy loss) or inelastic (having lost some energy). If energy is transmitted to the specimen, it may also result in the production of

Auger electrons or X-rays. Each of these events can provide information about the specimen [65].

In the SEM, an extremely focused electron beam strikes the object, causing the secondary electrons to be emitted from the sample. These electrons are collected by a detector, converted to a voltage, and amplified. The amplified voltage is applied to the grid of the cathode ray tube (CRT) and causes the intensity of the spot of light to change. The variations in the emission of secondary electrons are used to build up an image. The image consists of thousands of spots of varying intensity of the face of the CRT, corresponding to the topography of the specimen.

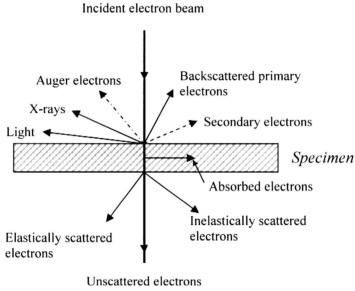

Fig. 4.6: Effects of electron-specimen interaction.

X-ray microanalysis makes use of the characteristic x-rays that are emitted from the sample when it is struck by electrons from an external source. Consequently, these x-rays are used to identify and quantify the elements that are present in an unknown sample. As can be seen in Fig. 4.7, incoming electrons interact with the inner shell

electrons of an atom, resulting in an electron being ejected from its shell, leaving the atom in an ionized position.

This instability is reduced if an electron from one of the higher energy outer shells falls to occupy the vacant position in the lower energy shell. This reduction in potential energy is released in the form of an x-ray. The energy of the x-ray produced is determined by the difference in energy between the sharply defined quantum energy levels in the atom. Because each atom has unique energy levels, the x-ray produced is thus characteristic of the atom from which it was emitted.

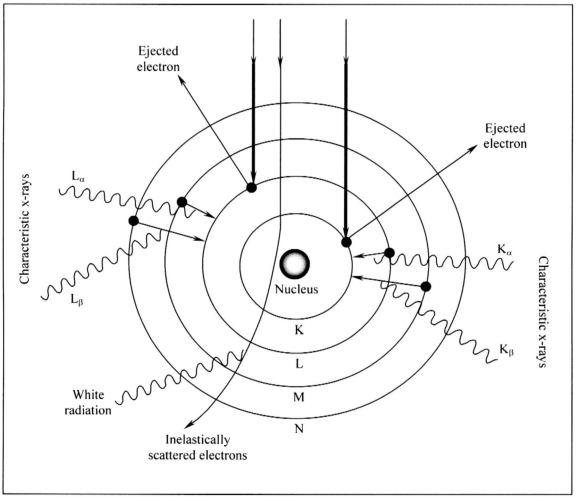

Fig. 4.7: Production of characteristic x-rays for EDS

The relationship between X-ray frequency ν (or energy) and atomic number Z was first proposed by Mosely [66] and is given by:

$$\nu = 0.248\ (Z-1)^2 \times 10^{16} \qquad \ldots\ldots \qquad \text{(Equation 4.3)}$$

The frequency ν of the X-ray radiation is related to its quantum energy E by the relationship E = hν where h is Planck's constant. The relationship between wavelength λ and energy is given by λ E = 12.4.

4.3.3 Sample Preparation

About 1g of powder was evenly dusted onto a 1cm length of a double-sided carbon tape, which was then attached to the surface of an aluminum specimen stub. A dryer was used to blow away excess powder. For non-conducting zeolite samples, a thin coating of conductive material was required. This was accomplished by depositing a thin layer of gold using a sputtering machine. The prepared stub was then placed onto the SEM stage in the microscope chamber for analysis (Fig. 4.8). The EDS analysis was performed on the same samples after SEM micrographs have been taken. The EDS sample area was representative of the area which appeared in the SEM micrographs.

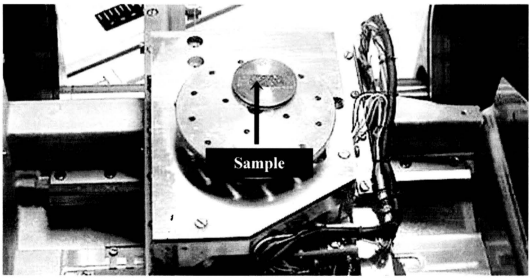

Fig. 4.8: The sampling chamber of the SEM

4.4 Transmission Electron Microscopy

4.4.1 Introduction

The main reason for utilizing the electron microscope is its superior resolution that result from the very small wavelengths as compared to other forms of radiation (such as light, x-rays and neutrons). The transmission electron microscope provides a sectional image of the sample, as opposed to the three-dimensional image obtained in SEM, which has a large depth of focus. However, the resolution of the TEM is better. These two types of microscopes thus complement each other. In this work, a Philips CM12 TEM (Fig. 4.9) operating at 80kV was used to examine samples produced.

Fig. 4.9: The Philips TEM used for observation of specimens.

4.4.2 Principle

The electrons that are needed to illuminate the specimen are produced by thermionic emission from an electron gun (usually a heated tungsten 'hairpin' filament or materials of lower work function such as lanthanum hexaboride). The position and inclination of the electron beam can be adjusted by suitable sets of magnetic alignment coils. The specimen to be observed is held in a special holder, and introduced into the high-vacuumed microscope chamber through an airlock [67]. The specimen is placed in the path of the electron beam, between the magnet lenses and the beam spreader, as illustrated in Fig. 4.10. These electrons are focused by a set of condenser lenses onto the specimen from the smallest possible spot, usually ~0.1μm, to the almost plane-parallel illumination of a large area. The phosphor-coated target will be illuminated in a greenish light, and the enlarged image of the thin film sample will be seen through the window.

4.4.3 Sample Preparation

About 20ml of deionized water is added to 0.5g of powder sample and kept in a closed glass vial. The mixture is dispersed by immersion into an ultrasonic bath for more than 48 hours until a fine suspension was formed. A drop of the resultant colloid is then placed onto a carbon-coated copper grid, and left to dry in a drying cabinet. The grid is then inserted into the TEM sample holder and placed on the TEM stage for observation.

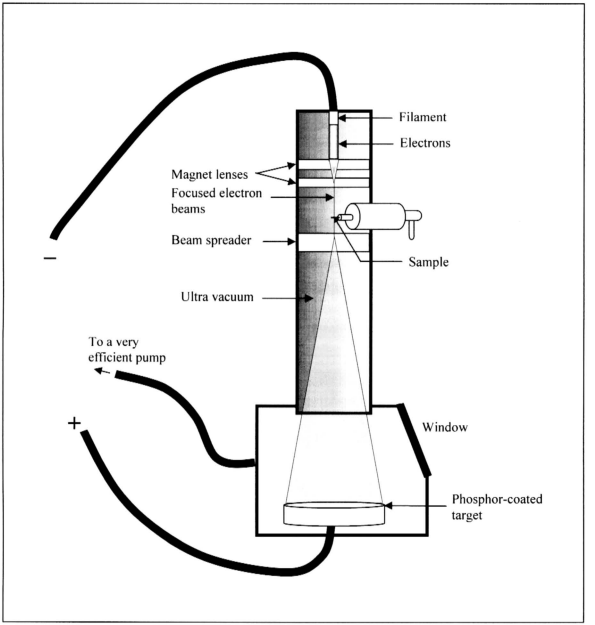

Fig. 4.10: A schematic representation of the TEM and the location of the sample.

4.5 Gas Adsorption Desorption

4.5.1 Introduction

Examination of powdered materials with electron microscopes do not disclose the internal structure of pores, their inner shape and dimensions, their volume and volume distribution, as well as their contribution to the surface area. By using gas adsorption, whereby each particle of the powder sample is enveloped in an adsorbed film, surface irregularities and pore interiors can be probed even at the atomic level [68]. The gas adsorption desorption measurements were conducted using a Sorptomatic 1990 Series from Thermo Finnigan (shown in Fig. 4.11).

4.5.2 Principle

The amount of vapor adsorbed on a solid surface depends on absolute temperature T, pressure P, and the interaction potential E between the adsorbate (vapor) and the adsorbent (surface). At an equilibrium pressure and temperature, the weight W of gas adsorbed on a unit weight of adsorbent is given by $W = f(P,E)$, if measurement is done at a constant temperature. A plot of W versus P at constant T is referred to as the adsorption isotherm of a particular vapor-solid interface. E varies with the properties of different adsorbates and adsorbents. Physical, or reversible adsorption is more suitable for surface area determination compared with chemical adsorption (chemisorption) because:

(a) it is accompanied by low heats of adsorption with no disruptive structural changes to the surface,

(b) the surface is covered by more than one layer of adsorbates so that pores can be filled for volume measurements, and

(c) the process is fully reversible, enabling both the adsorption and desorption processes to be studied [69].

The desorption isotherm may be considered to be a record of the removal of gas from the sample and as such is the reverse of the adsorption isotherm. The sample must initially be saturated with gas before the full desorption isotherm can be measured. The desorption isotherm often follows a different path from the adsorption isotherm yielding a hysteresis loop; its shape indicates something about the complexity and shape of the pores within the sample. Pore size distribution can be calculated from both the adsorption and desorption isotherms, according to preference; both will give different results if a hysteresis loop is present.

The Barrett, Joyner, and Halenda (BJH) numerical integration method is used to calculate the pore size distribution [70]. It takes advantage of Wheeler's theory that condensation occurs in the pores when a critical relative pressure is reached which corresponds to the Kelvin radius r_k. The BJH method also assumes a multilayer of adsorbed film with a depth of t exists on the pore wall when evaporation or condensation occurs which is of the same depth as the adsorbed film on a nonporous surface.

The Brunauer-Emmett-Teller (BET) method was also used to calculate specific surface areas of the powdered samples. This method involves the determination of the amount of the adsorbate required to cover the external and the accessible internal pore surfaces of a solid with a complete monolayer of adsorbate. The specific surface area, A_{sp} can be calculated from the results of BET measurements.

4.5.3 Sample Preparation

First an empty sample tube was weighed. Next, about 0.05-0.5g of sample was inserted into the sample tube. After a degassing procedure, in which moisture was removed, the sample tube containing the sample was weighed again. The sample tube was then inserted into the Sorptomatic chamber. The measurement was begun when a steady flow of nitrogen gas was flowed into the sample tube. The maximum adsorption pressure was set at 1000 mm Hg because of the microporous nature of the zeolite samples.

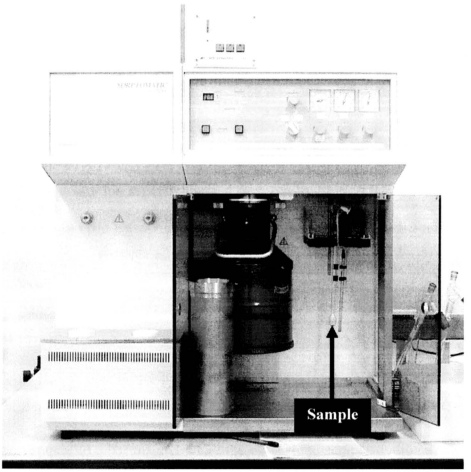

Fig. 4.11: The Sorptomatic machine used for gas adsorption desorption measurements.